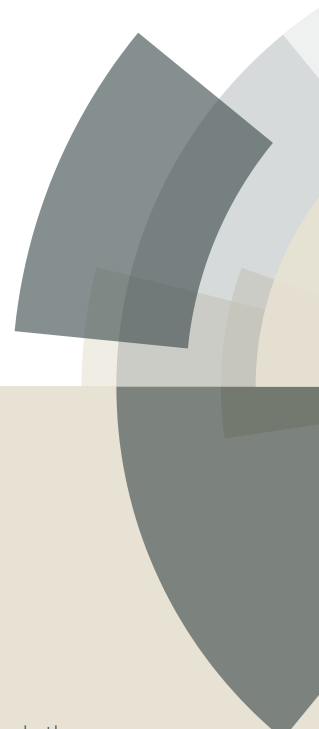


PCCP

Accepted Manuscript



This article can be cited before page numbers have been issued, to do this please use: G. Horvat, L. Erkanec, N. Cindro and V. Tomisic, *Phys. Chem. Chem. Phys.*, 2017, DOI: 10.1039/C7CP03920D.



This is an Accepted Manuscript, which has been through the Royal Society of Chemistry peer review process and has been accepted for publication.

Accepted Manuscripts are published online shortly after acceptance, before technical editing, formatting and proof reading. Using this free service, authors can make their results available to the community, in citable form, before we publish the edited article. We will replace this Accepted Manuscript with the edited and formatted Advance Article as soon as it is available.

You can find more information about Accepted Manuscripts in the [author guidelines](#).

Please note that technical editing may introduce minor changes to the text and/or graphics, which may alter content. The journal's standard [Terms & Conditions](#) and the ethical guidelines, outlined in our [author and reviewer resource centre](#), still apply. In no event shall the Royal Society of Chemistry be held responsible for any errors or omissions in this Accepted Manuscript or any consequences arising from the use of any information it contains.

A comprehensive study of alkali metal cations complexation by lower rim calix[4]arene amide derivatives

Gordan Horvat,^{*a} Leo Frkanec,^b Nikola Cindro^a and Vladislav Tomišić^{*a}

^a Division of Physical Chemistry, Department of Chemistry, Faculty of Science, University of Zagreb, Horvatovac 102a, 10000 Zagreb, Croatia

^b Laboratory for Supramolecular Chemistry, Division of Organic Chemistry and Biochemistry, Ruđer Bošković Institute, Bijenička cesta 54, 10000 Zagreb, Croatia

Abstract

Complexation of alkali metal cations by lower rim *N,N*-dihexylacetamide (**L1**) and newly synthesized *N*-hexyl-*N*-methylacetamide (**L2**) calix[4]arene tertiary-amide derivatives was thoroughly studied at 25 °C in acetonitrile (MeCN), benzonitrile (PhCN), and methanol (MeOH) by means of direct and competitive microcalorimetric titrations, as well as UV and ¹H NMR spectroscopies. In addition, by measuring ligands solubilities, solution (transfer) Gibbs energies of the ligands and their alkali metal complexes were obtained. The inclusion of solvent molecules in the free and complexed calixarene hydrophobic cavity was also investigated. Computational (classical molecular dynamics) investigations of the studied systems were carried out as well. The obtained results were compared with those previously obtained by studying complexation abilities of *N*-hexylacetamidocalix[4]arene secondary-amide derivative (**L3**). The stability constants of 1:1 complexes were determined in all solvents used (the values obtained by different methods being in excellent agreement), as were the corresponding complexation enthalpies and entropies. Almost all of the examined reactions were enthalpically controlled. The most striking exceptions were reactions of Li⁺ with both ligands in methanol, for which entropic contribution to the reaction Gibbs energy was substantial due the entropically favourable desolvation of the smallest lithium cation. Thermodynamic stabilities of the complexes were quite solvent dependent (stability decreased in the solvent order: MeCN > PhCN >> MeOH), which could be accounted for by considering the differences in the solvation of the ligand as well as free and complexed alkali metal cations in the solvents used. Comparison of the stability constants of ligands **L1** and **L2** complexes clearly revealed that higher electron-donating ability of the hexyl with respect to methyl group is of considerable importance in determining the equilibria of the complexation reactions. Additionally, the quite strong influence of intramolecular hydrogen bonds formation in compound **L3** (not present in ligands **L1** and **L2**) as well that of inclusion of solvent molecules into the calixarene hydrophobic *cone* were shown to be of great importance in determining the calixarene-cation complex thermodynamic stability. The experimental results were fully supported by those obtained by MD simulations.

* Authors to whom correspondence should be addressed (E-mail: ghorvat@chem.pmf.hr, vtomistic@chem.pmf.hr)

1. Introduction

Calixarenes are macrocyclic ligands which, when substituted at the upper and/or lower rim, can efficiently and in some cases selectively bind cations, anions, and neutral molecules.^{1–5} Due to the specific spatial arrangement of phenolic subunits in these compounds, a well-defined binding site can be achieved by introducing substituents with appropriate functional groups.^{6–10} The lower rim derivatives comprising carbonyl functional groups, i.e. ketones, esters, or amides, have been extensively studied and were shown to form quite stable complexes with alkali-, alkaline-earth, and transition-metal cations in various solvents.^{7,8,10–12} In such compounds a cation-binding site is formed by nucleophilic ether and carbonyl oxygen atoms. Particularly interesting derivatives are those which bear secondary- and tertiary-amide substituents at the lower rim due to their high, but mutually quite different affinities towards alkali metal cations.^{13–27} The difference in the stabilities of the corresponding complexes is mostly a consequence of the fact that secondary-amide derivatives are able to form intramolecular N–H···O=C hydrogen bonds, which significantly decrease their abilities to bind cations as compared to tertiary-amide derivatives.^{14,18,27–29}

The calixarene cation-binding ability is in general rather strongly influenced by the compatibility of the sizes of cation and ligand-binding site. In addition, solvation of reactants and products of the complexation reaction plays a very important role in the binding process. In this respect, the inclusion of solvent molecules in the calixarene hydrophobic *cone* can be of great importance.^{4,16,23,24,30–32} This specific interaction with solvent molecules is facilitated by cation binding which leads to an appropriate ligand's *cone* preorganization. It has been shown that such an inclusion of solvent molecule can significantly increase the cation-calixarene complex thermodynamic stability.^{16,23,24,33}

As already mentioned, calixarene amides have been known as very efficient binders of alkali metal cations. However, the factors governing this efficiency, e.g. the nature of substituents at the amide groups and solvation effect, have not been fully explored. Recently we have reported on detailed thermodynamic, structural, and computational studies of the complexation reactions of a secondary-amide calix[4]arene derivative **L3** (Fig. 1) with alkali metal cations in several solvents.^{16,23} In this paper we present the investigations of complexation affinities of two tertiary-amide calixarene derivatives **L1** and **L2** (Fig. 1) towards alkali metal cations. In order to explore the solvent effect on the equilibria of complexation reactions, three solvents were used, namely acetonitrile, benzonitrile, and methanol. The solvents were chosen considering differences in their cation and ligands solvation abilities as well as affinities for hydrogen bonding and for inclusion in the calixarene *basket*. Stability constants of the complexes, as well as complexation enthalpies and entropies, were determined by means of direct and competitive microcalorimetric titrations (the latter were necessary because of the high complex stabilities). In some cases complexation reactions were also quantitatively studied spectrophotometrically. A detailed structural insight into the alkali

metal cations complexation by ligands **L1** and **L2**, as well as into the solvent-molecule inclusion in the hydrophobic calixarene cavity, was achieved by ^1H NMR measurements and molecular dynamics simulations. The obtained thermodynamic results are thoroughly discussed and compared to those corresponding to compound **L3** regarding structural characteristics of the ligands. The solvent effect, *i.e.* that of reactants and product solvation, on the complexation reactions has been particularly addressed.

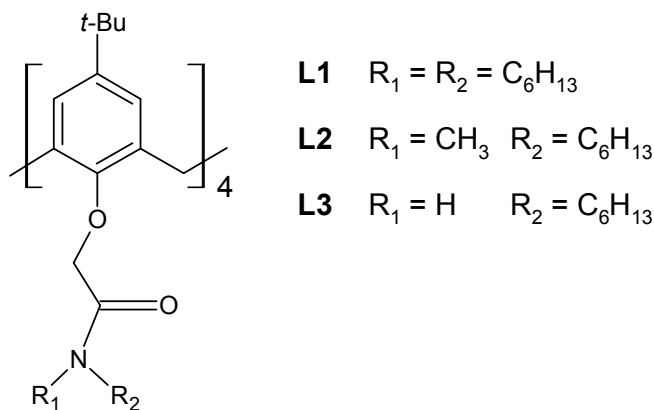


Fig. 1 Structures of compounds **L1** to **L3**.

2. Experimental

2.1 Synthesis

Compounds **L1** and **L3** and the acid chloride of calix[4]arene tetracetic acid (the *cone* conformer) were prepared according to the procedures described elsewhere.²¹

5,11,17,23-Tetra-*tert*-butyl-25,26,27,28-tetrakis(*N*-hexyl-*N*-methyl-carbamoylmethoxy)calix[4]arene (**L2**)

Tetraacid (1.00 g, 1.13 mmol) and thionyl chloride (5.0 mL) were refluxed for one hour, evaporated and then coevaporated with dry toluene. Resulting acyl-chloride was dissolved in 50 mL of dry DCM and cooled under argon to 0 °C. With vigorous stirring mixture of pyridine (1.00 mL, 12.9 mmol) and *N*-hexylmethylamine (0.86 mL, 5.7 mmol) dissolved in 10 mL of dry DCM was added dropwise. Mixture was stirred for 24 hours, diluted with DCM, washed 5 times with miliQ water and evaporated without drying. Crude compound was dissolved in 20 mL of boiling HPLC grade acetonitrile and left to crystalize in refrigerator, yielding 570 mg (40 %) of pure compound. Analytically pure sample was obtained by recrystallization (again from acetonitrile).

Following signals were found in the ^1H NMR and ^{13}C NMR spectra of NaL2^+ complex in CDCl_3 :

^1H NMR (CDCl_3) δ/ppm 7.14 (s, 8H), 4.63-4.38 (m, 12H), 3.46-3.27 (m, 8H), 3.12 (bs, 4H), 3.01-2.86 (m, 12H), 1.58 (bs, 8H), 1.40-1.24 (m, 24H), 1.17 (s, 36H), 0.94-0.83 (m, 12H);

^{13}C NMR (CDCl_3) δ/ppm 168.67 (s), 168.55 (s), 151.36 (s), 151.24 (s), 151.08 (s), 150.86 (s), 148.08 (s), 135.03 (s), 125.78 (d), 117.11 (s), 74.09 (t), 73.97 (t), 48.55 (t), 48.35 (t), 48.16 (t), 34.28 (t), 33.86 (q), 33.24 (q), 31.90 (t), 31.60 (t), 31.39 (q), 30.19 (t), 28.19 (t), 27.37 (t), 26.99 (t), 26.48 (t);

The structure of the **L2** ligand was confirmed by HRMS (MALDI-TOF) spectrometry: m/z $[\text{M} + \text{H}^+]^-$ calculated for $((\text{C}_{20}\text{H}_{31}\text{O}_2\text{N})_4)^-$ – 1269,9497, found 1269,9474.

2.2 Materials for physicochemical measurements

The solvents, acetonitrile (MeCN, Merck, Uvasol and J. T. Baker, HPLC grade), benzonitrile (Sigma Aldrich, Chromasolv, 99.9 %), and methanol (J. T. Baker, HPLC grade) were used without further purification. The salts used for the investigation of **L** complexation were LiClO_4 (Sigma Aldrich, 99.99 %), NaClO_4 (Sigma Aldrich, 98+ %), KClO_4 (Merck, *p.a.*), KSCN (Sigma Aldrich, ≥ 99 %), RbCl (Sigma Aldrich, 99 %), RbBPh_4 (Sigma Aldrich, 95 %), CsCl (Sigma Aldrich, 99.5 %).

2.3 Solubility determinations

Saturated solutions of **L1** and **L2** in acetonitrile and methanol were prepared by adding an excess amount of the solid substance to the solvent. The obtained mixtures were left in a thermostat at 25 °C for several days in order to equilibrate. The concentrations of saturated solutions were determined at 25.0 °C spectrophotometrically by means of a Varian Cary 5 spectrophotometer equipped with a thermostating device. Calibration curves were obtained by measuring the absorbances of **L1** and **L2** solutions of known concentrations.

2.4 Spectrophotometry

UV titrations of **L1** and **L2** with alkali metal salt solutions in acetonitrile and methanol were performed at (25.0 ± 0.1) °C by means of a Varian Cary 5 spectrophotometer. The metal salt solutions were added to a solutions of ligands' placed in the quartz cell ($l = 1$ cm or $l = 10$ cm). After each addition UV spectrum was recorded with a sampling interval of 1 nm and integration time of 0.2 s. The stability constant of the complexation of cesium cation with **L1** in acetonitrile was determined by spectrophotometric titrations (Table 1, Fig. 7). Due to the rather small affinity of **L1**

towards Cs^+ cation, the largest concentration of cesium salt solution that was prepared was insufficient to ensure the reliable determination of CsL1^+ complex stability constant by a titration in which the titrant was the metal salt solution. For that reason, the titration was performed in a way that the concentration of cesium cation was varied by the removal of a certain volume of the reaction mixture that contained **L1** and Cs^+ cation which was replaced by the same volume of **L1** solution of the exact analytical concentration as the one in the reaction cell. By this method it was possible to reach an adequate range of analytical concentration of Cs^+ and, in return, determine a reliable value of the CsL1^+ stability constant. The value of stability constant of RbL2^+ complex was determined using cuvettes with a 10 cm optical path that enabled the measurements of reaction mixture spectra in an adequate range of analytical concentrations of **L2** for a reliable stability constant determination. All measurements were done in triplicate. The obtained data were analyzed by multivariate non-linear regression analysis using Hyperquad program.³⁴

2.5 ^1H NMR and ^{13}C NMR studies

^1H NMR titrations were carried out at 25 °C by means of a Bruker Avance 600 MHz with a solvent signal used as standard for titrations in CD_3CN and CD_3OD or with a TMS signal as standard in CDCl_3 solutions. In titrations of **L1** and **L2** with the alkali metal cations in deuterated acetonitrile, the solutions salts were added to the solutions of **L1** and **L2**. Spectra were recorded at 32 pulses.

^1H and ^{13}C NMR spectra of NaL2^+ complex (Fig. S1, ESI) were recorded on Bruker Ascend 400 MHz at rt using TMS as a reference in proton spectra and middle signal of CDCl_3 (77.16 ppm) in carbon spectra, chemical shifts are reported in ppm.

Solutions of LiL2^+ , NaL2^+ and KL2^+ complexes in CDCl_3 were prepared by dissolving ligand in deuterated chloroform followed by the addition of appropriate metal salt solid. Sonification of the solutions was used to ensure complete complexation.

2.6 Mass spectrometry

HRMS spectrum of **L2** was obtained on a Bruker Microflex MALDI / TOF instrument.

2.7 Calorimetry

Microcalorimetric measurements were conducted with an isothermal titration calorimeter Microcal VP-ITC at 25.0 °C. The calorimeter was calibrated electrically, and its reliability was additionally checked by carrying out the complexation of barium(II) by 18-crown-6 in aqueous medium at 25 °C. The results obtained ($\log K = 3.75$, $\Delta_r H = -31.7 \text{ kJ mol}^{-1}$) were in excellent agreement with the

literature values ($\log K = 3.73$, $\Delta_r H = -31.5 \text{ kJ mol}^{-1}$).³⁵ Thermograms were processed using the Microcal OriginPro 7.0 program.

In the calorimetric studies of alkali metal cations complexation by **L**, the enthalpy changes were recorded upon stepwise additions of acetonitrile, benzonitrile or methanol solution of metal salt into solution of ligand ($V_0 = 1.4182 \text{ cm}^3$). Titrations of the M-L1^+ and M-L2^+ complexes with acetonitrile in benzonitrile were carried out by the addition of MeCN solution in PhCN to the solution of complexes in the same solvent. The heats measured in the titration experiments were corrected for heats of titrant dilution obtained by blank experiments. The dependence of successive enthalpy changes on the titrant volume was processed by non-linear least-squares fitting procedure using OriginPro 7.5 program. All measurements were repeated three or more times.

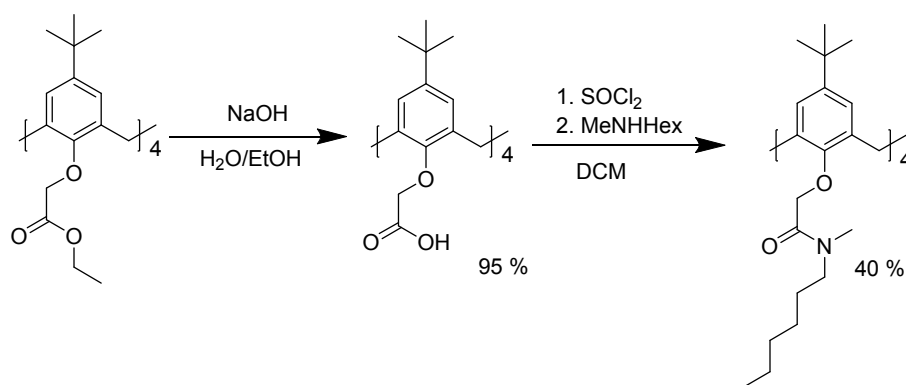
2.8 Molecular dynamics simulations

The molecular dynamics simulations were carried out by means of the GROMACS³⁶⁻⁴² package (version 5.1.4). Intramolecular and nonbonded intermolecular interactions were modelled by the OPLS-AA (Optimized Parameters for Liquid Simulations-All Atoms) force field.⁴³ Partial charges assigned to ring carbons bound to CH_2 groups that link the monomers were assumed to be zero. The initial structures of ligands **L1** and **L2**, as well as their alkali metal complexes, were derived from the crystal structure of sodium complex of similar secondary amide calixarene derivative.²³ The calixarene ligands, their alkali metal complexes and corresponding acetonitrile adducts were solvated in cubical boxes containing between 2100 and 3700 molecules of acetonitrile, benzonitrile or methanol, and with periodic boundary conditions. The solute concentration in such a box was about 0.01 mol dm^{-3} . The solvent boxes were equilibrated prior to inclusion of ligands and their complexes with the box density after equilibration in all cases being close to the experimental one within 2 %. During the simulations of the systems comprising calixarene and metal cations, Cl^- ion was included to neutralize the box. The chloride counterion was kept fixed at the box periphery whereas the complex was initially positioned at the box center. In all simulations an energy minimization procedure was performed followed by a molecular dynamics simulation in NpT conditions for 50.5 ns, where the first 0.5 ns were not used in data analysis. The Verlet algorithm⁴⁴ with a time step of 1 fs was employed. The cutoff radius for nonbonded van der Waals and short-range Coulomb interactions was 16 Å. Long-range Coulomb interactions were treated by the Ewald method as implemented in the PME (Particle Mesh Ewald) procedure.⁴⁵ The simulation temperature was kept at 298 K with the Nosé-Hoover^{46,47} algorithm using a time constant of 1 ps. The pressure was kept at 1 bar by Martyna-Tuckerman-Tobias-Klein⁴⁸ algorithm and the time constant of 1 ps. Figures of calixarene molecular structures were created using VMD software.⁴⁹

3. Results and discussion

3.1 Synthesis

Compound **L2** was synthesized according to the previously described method, starting from the corresponding tetraester which was hydrolyzed to tetraacid. In reaction with thionyl chloride tetrachloride was obtained which was reacted with excess of *N*-methylhexylamine to yield the target compound (Scheme 1).



Scheme 1 Synthesis of compound **L2**.

3.2 Structural studies of **L1** and **L2** in solution

Molecular structures of ligands **L1** and **L2** in solution were studied by means of ¹H NMR spectroscopy and MD simulations. In the ¹H NMR spectrum of **L1** in CDCl₃ (Fig. 2, Table S1, ESI) a single set of ligand proton signals (*tert*-butyl, Ar-H, and Ar-O-CH₂ proton singlets and two doublets for equatorial and axial protons) is present. Such a signal pattern is characteristic for C₄ cone conformation, or represents dynamic C₂-C₂ cone exchange that is fast on the ¹H NMR time scale.⁵ The spectra of **L1** in CD₃CN and CD₃OD are similar to that in CDCl₃ in terms of proton-signal multiplicity. However, in acetonitrile the signal of Ar-H protons is significantly downfield shifted compared to chloroform and methanol (Fig. 2, Table S1, ESI). This is usually considered as an indication of the inclusion of acetonitrile molecule into the hydrophobic calix[4]arene hydrophobic cavity^{18,24,50} which is fast on the ¹H NMR time scale.

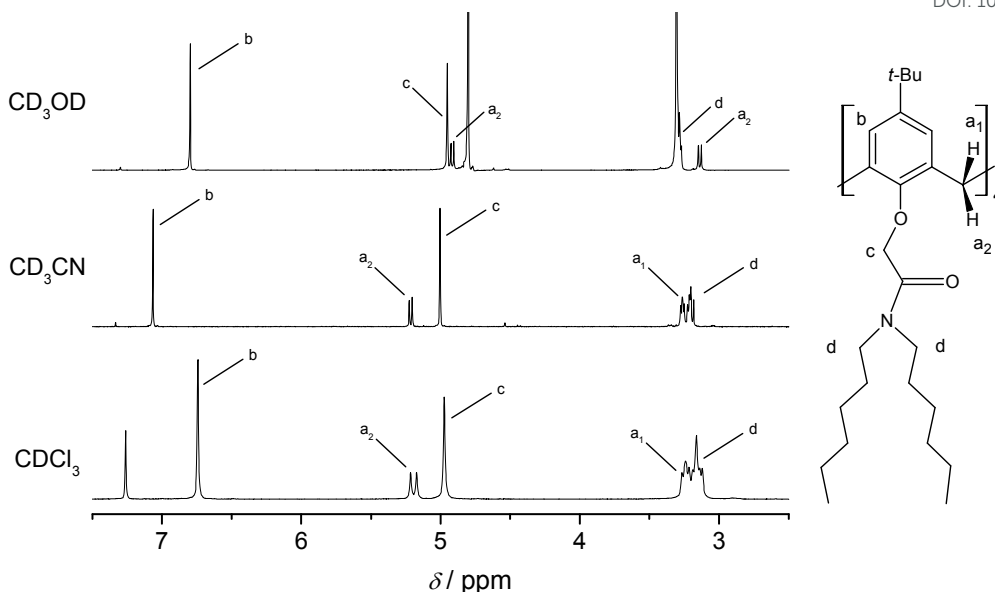


Fig. 2 ^1H NMR spectra of **L1** in deuterated chloroform, acetonitrile, and methanol at 25 °C.

Ligand **L2** is asymmetrically substituted tertiary-amide calix[4]arene derivative in which a rotational isomerism is possible regarding the orientation of methyl and hexyl substituents with respect to the amide oxygen atom, the corresponding reorientation activation enthalpy being ≈ 70 kJ mol $^{-1}$.⁵¹ As a consequence, the rotation is relatively slow at room temperature at the ^1H NMR timescale, leading to an appearance of separate proton signals for each of the rotamers. There are 6 different rotamers of **L2** possible in C_4 cone conformation and 9 rotamers when calixarene basket is in flattened cone conformation of C_2 symmetry. In ^1H NMR spectra of **L2** in CD_3Cl there are between 9 and 11 signals present for each of the ligand's proton type (Fig. 3), where the most notable differences in relative chemical shifts were found for aromatic and *tert*-butyl protons. Similar phenomenon was observed in the spectra of **L2** in deuterated acetonitrile, methanol, and dimethyl sulfoxide (Fig. 3). Upon temperature increase of dimethyl sulfoxide **L2** solution from 25 °C to 100 °C, multiple signals collapsed into a single one (Fig. 4). The above findings can be explained by taking into account a possibility of the existence of an equilibrium between **L2** rotamers, each having different set of proton signals. Again a chemical shift of Ar-H protons in CD_3CN is considerably higher than in CDCl_3 and CD_3OD , indicating a possible inclusion of acetonitrile molecule into the hydrophobic **L2** basket. Due to the complexity of **L2** spectrum in CD_3CN , and the fact that Ar-H proton shifts lie somewhere between values of those corresponding to the free **L1** and **L1MeCN** species, it was not possible to elucidate with certainty whether **L2MeCN** adduct is present in the acetonitrile solution of **L2**.

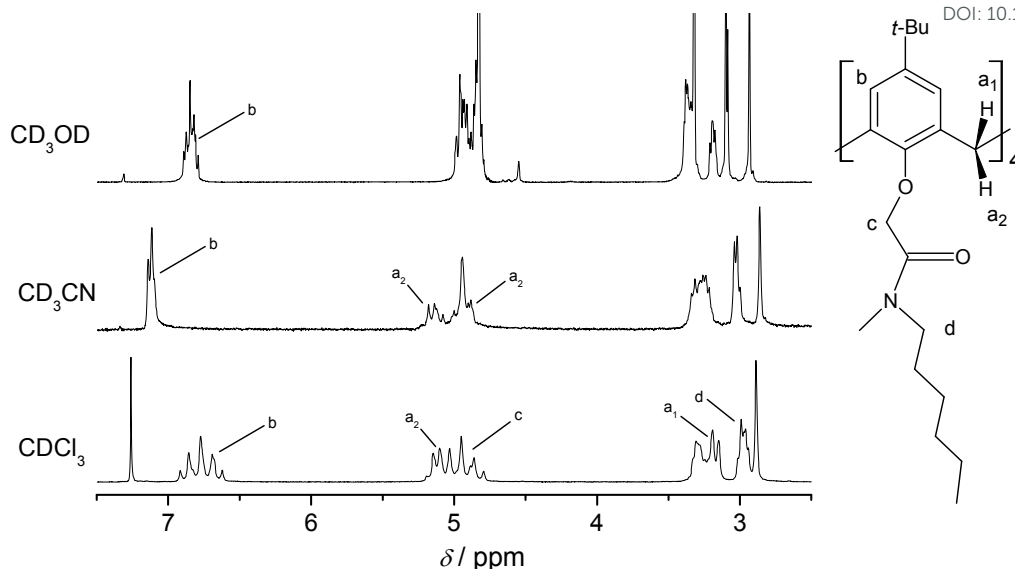


Fig. 3 ^1H NMR spectra of **L2** in deuterated chloroform, acetonitrile, and methanol at 25 °C.

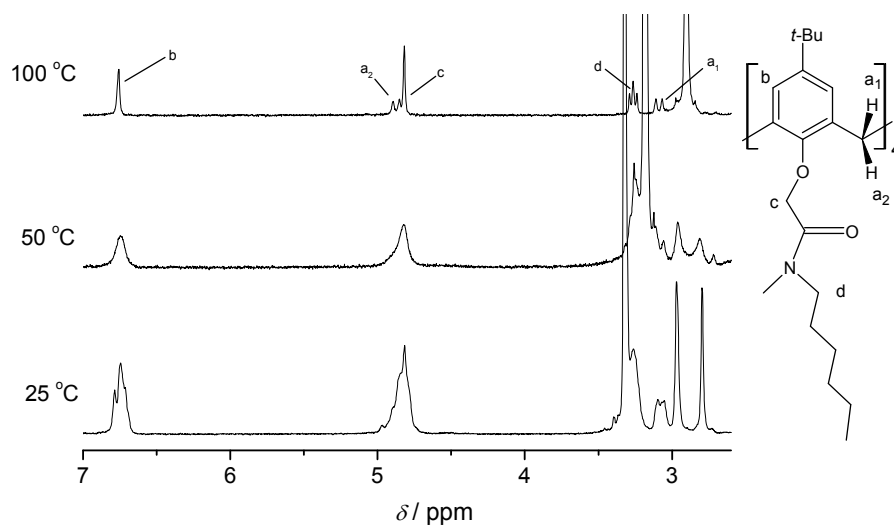


Fig. 4 Temperature dependence of **L2** ^1H NMR spectrum in deuterated dimethyl sulfoxide.

The structures of calixarene ligands **L1** and **L2** were also investigated by molecular dynamics simulations. Due to the existence of several rotamers of **L2**, two isomers with most distinct structural features were simulated, **Z-L2** in which carbonyl oxygen atom lie on the same side of amide bond as hexyl group in all four calixarene subunits, and **E-L2** with the opposite orientation of the named groups at the calixarene lower rim (Figs. S2 and S3, ESI). During simulations in acetonitrile, an inclusion of solvent molecules in the calixarene *basket* was observed for both ligands (Figs. S2 and S3, ESI). This process had an influence on the shape of the calixarene *cone* which changed from the flattened to the regular one upon MeCN molecule inclusion. On the other hand, the

inclusion of benzonitrile molecule in the free ligands was not observed during MD simulations in that solvent.

3.3 Studies of alkali metal cations complexation in acetonitrile

Stability constants of **L1** and **L2** complexes with alkali metal cations were determined by means of microcalorimetric and spectrophotometric titrations (Table 1). Due to the large affinities of the studied macrocycles for Li^+ , Na^+ , and K^+ cations, the determination of the corresponding equilibrium constants was not possible by direct calorimetric titrations. Therefore, these constants, along with the corresponding reaction enthalpies and entropies, were determined by means of displacement microcalorimetric titrations. The values of complexation thermodynamic quantities were obtained by the combination of the results of competition titrations and those obtained by direct titrations of ligands **L1** and **L2** with rubidium cation (Fig. 5 and S5, ESI). The stability constants of complexes of both ligands with potassium cation were determined from the titration of solution of rubidium complex with the solution of potassium cation (Fig. 6 and S20, ESI). The equilibrium constants for the formation of sodium complexes were determined from the results of the displacement titration of potassium complexes with sodium cation solution (Figs. S6 and S21, ESI). The affinities of both ligands for Na^+ were greater than for Li^+ , so the stability constants of LiL1^+ and LiL2^+ complexes were determined by the competition microcalorimetric titration of lithium complex solution with sodium cation solution (Figs. S7 and S22, ESI). Due to the difference in the stabilities of LiL^+ and KL^+ complexes, a more adequate procedure to determine the equilibrium constants of complexation of **L1** and **L2** with lithium cation would be by means of displacement titrations of the complexed potassium cation with Li^+ . However, the similar values of reaction enthalpies for the complexation of the studied ligands with these cations cause a rather small heat effect due to the cation substitution, which then lead to unreliable experimental data.

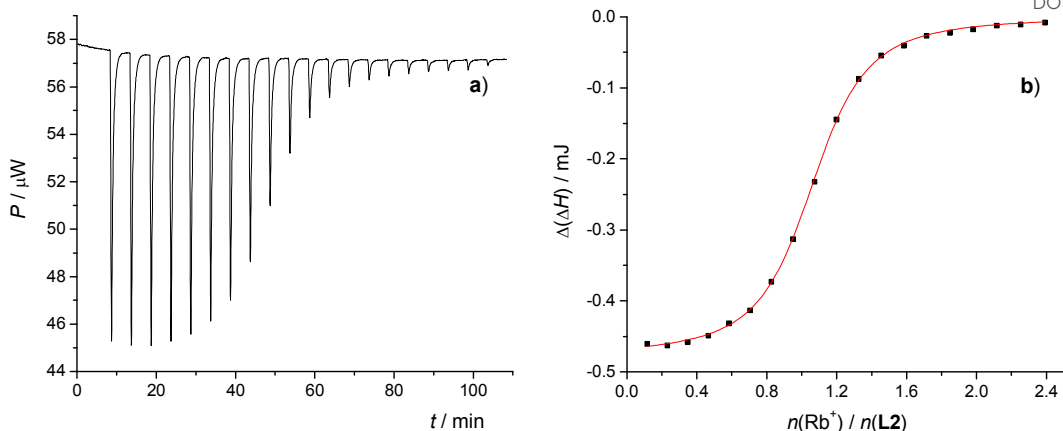


Fig. 5 a) Microcalorimetric titration of **L2** ($c = 9.95 \times 10^{-5} \text{ mol dm}^{-3}$, $V = 1.4182 \text{ cm}^3$) with RbNO_3 ($c = 1.07 \times 10^{-3} \text{ mol dm}^{-3}$) in acetonitrile; $t = 25 \text{ }^\circ\text{C}$; b) Dependence of successive enthalpy change on $n(\text{Rb}^+)/n(\text{L2})$ ratio. ■ experimental; — calculated.

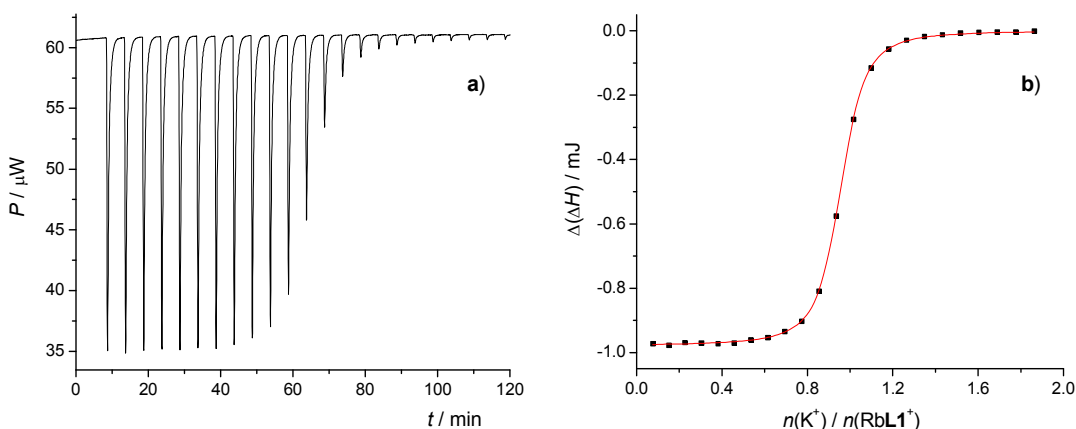


Fig. 6 a) Microcalorimetric titration of RbL1^+ ($c = 4.95 \times 10^{-4} \text{ mol dm}^{-3}$, $V = 1.4182 \text{ cm}^3$) with KClO_4 ($c = 5.23 \times 10^{-3} \text{ mol dm}^{-3}$) in acetonitrile; $t = 25 \text{ }^\circ\text{C}$; b) Dependence of successive enthalpy change on $n(\text{K}^+)/n(\text{RbL1}^+)$ ratio. ■ experimental; — calculated.

The complexation reaction enthalpies were also determined by direct titrations. As can be seen from the data listed in Table 1 and Table S4, ESI, the values obtained by direct and displacement titrations are in very good agreement. This fact can serve as a confirmation of the reliability of the thermodynamic results obtained in this work.

All complexation reactions are enthalpically controlled, whereby the absolute entropic contribution to the standard reaction Gibbs energy is approximately an order of magnitude smaller in comparison to the enthalpic contribution for all complexes, except those with lithium cation. The latter can be explained by considering that due to the strong solvation of this cation in acetonitrile, its desolvation entropy is more favorable than for the other cations.¹⁸ It should be noted that the stability

constants of **L1** and **L2** complexes with alkali metal cations in acetonitrile are about 5 orders of magnitude larger than those corresponding to the secondary amide derivative **L3**.²³ As already mentioned, this difference in ligand affinities is mainly due to the enthalpically unfavorable disruption of intramolecular hydrogen bonds network in **L3** in the course of cation coordination by carbonyl oxygen atoms. Such an effect is clearly reflected in the values of reaction enthalpies, which are between 28 kJ mol⁻¹ and 35 kJ mol⁻¹ more negative for the cation complexation by ligands **L1** and **L2** compared to that of **L3**. Compounds **L1** and **L2** have similar affinities towards Li⁺ and Na⁺ cations, although reaction enthalpies for the formation of Li**L2**⁺ and Na**L2**⁺ complexes are about 5 kJ mol⁻¹ larger than for the formation of Li**L1**⁺ and Na**L1**⁺. These differences in reaction enthalpies are somewhat compensated with more favorable entropic contributions in the cases of alkali metal cation complexation reactions with **L2** compared to **L1**.

The differences in affinities of **L1** and **L2** for potassium and rubidium cations are more pronounced than in the case of Li⁺ and Na⁺, i.e. **L1** binds former cations significantly more strongly than **L2**. The reaction enthalpies of K⁺ and Rb⁺ complexation with **L1** are about 5 kJ mol⁻¹ lower than the ones corresponding to **L2**, which in turn impacts the overall stability of the complexes formed. Such an effect is most probably the result of the different electron-donating character of methyl and hexyl substituents bound to the amide groups, i.e. hexyl group is better electron donor than methyl one.⁴

Table 1 Thermodynamic parameters for complexation of alkali metal cations with **L1** and **L2** in acetonitrile at 25 °C determined by microcalorimetric and spectrophotometric titrations.

Cation	log <i>K</i> ± SE	(Δ _r <i>G</i> ^o ± SE) kJ mol ⁻¹	(Δ _r <i>H</i> ^o ± SE) kJ mol ⁻¹	(Δ _r <i>S</i> ^o ± SE) J mol ⁻¹ K ⁻¹
L1				
Li ⁺	11.27 ± 0.06	-64.3 ± 0.4	-53.7 ± 0.3	36.4 ± 3.2
Na ⁺	12.15 ± 0.04	-69.4 ± 0.2	-70.3 ± 0.3	-3.1 ± 1.0
K ⁺	9.19 ± 0.02	-52.5 ± 0.1	-54.1 ± 0.3	-5.5 ± 0.9
Rb ⁺	6.39 ± 0.02	-36.5 ± 0.1	-35.3 ± 0.3	3.8 ± 0.8
Cs ⁺	3.69 ± 0.01 ^a	-21.06 ± 0.05		
L2				
Li ⁺	11.09 ± 0.01	-63.3 ± 0.1	-48.8 ± 0.2	48.4 ± 0.8
Na ⁺	12.27 ± 0.01	-70.0 ± 0.1	-64.6 ± 0.2	18.0 ± 0.8
K ⁺	8.46 ± 0.01	-48.2 ± 0.1	-48.6 ± 0.2	-1.1 ± 0.8
Rb ⁺	5.61 ± 0.01	-31.99 ± 0.08	-29.9 ± 0.2	6.9 ± 0.7
	5.690 ± 0.007 ^a			

^a determined spectrophotometrically. SE = standard error of the mean (*N* = 3–5).

Spectrophotometric titrations of ligands **L1** and **L2** in acetonitrile were also conducted. In all of the titrations the addition of salt solution resulted in the decrease of absorbance in the larger part of the ligand UV spectrum. In the cases of titrations with lithium, sodium, potassium and rubidium cations, there was no change of the solution spectrum after the equimolar cation/ligand ratio (Figs. S8–S11, S23–S25, ESI). That indicated strong complexation and formation of complexes with 1:1 stoichiometry, in accordance with the result of microcalorimetric measurements. Stability constants of CsL1^+ and RbL2^+ (Table 1) were calculated by processing spectrophotometric data collected in a way described in the Experimental section (Fig. 7 and S26, ESI).

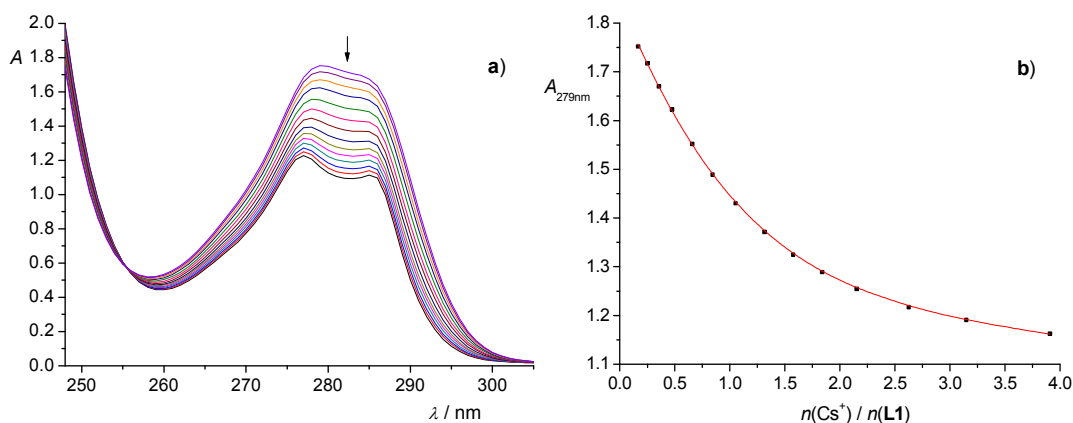


Fig. 7 a) Spectrophotometric titration of **L1** ($c = 3.81 \times 10^{-4} \text{ mol dm}^{-3}$, $V_0 = 2.5 \text{ cm}^3$) with CsNO_3 in acetonitrile. $l = 1 \text{ cm}$, $t = 25.0 \text{ }^\circ\text{C}$. b) Dependence of absorbance at 279 nm on $n(\text{Cs}^+) / n(\text{L1})$ ratio. ■ experimental; — calculated.

In order to assess the structure of alkali metal cation complexes in acetonitrile, ^1H NMR titrations were carried out. When **L1** was titrated with alkali metal cation solutions the observed changes in ^1H NMR spectra were similar in all cases (Figs. S12–S15, ESI). Namely, the ion exchange was slow on the ^1H NMR time scale leading to the appearance of two distinct sets of signals, one that can be attributed to the free **L1** and the other assigned to the complexed form of the calixarene ligand. From the obtained results it cannot be ascertained whether or not the formed complexes contained specifically bound acetonitrile molecule in their hydrophobic cavities, as was the case for lithium, sodium, and potassium complexes of **L3** in acetonitrile.²³ Titration of **L2** with alkali metal cation solutions in CD_3CN led to the unification of several proton signals of Ar-H and *tert*-butyl protons of free **L2** (Figs. S27–S30, ESI) into one signal for each proton, separate from the original signals, which was an indicator of a slow cation exchange on the ^1H NMR timescale. Newly emerged signals were assigned to the **L2**-cation complex for all cations studied. The reduction of a number of upper-rim proton signals can be rationalized by the symmetrization of calixarene *basket*

upon cation binding into a C_4 conformation, a conformational transition already experimentally and computationally observed for calix[4]arene amide derivatives.²³ A similar effect can be seen in the ^1H NMR spectra of **L2** complexes with Li^+ , Na^+ and K^+ cations in deuterated chloroform (Fig. 8).

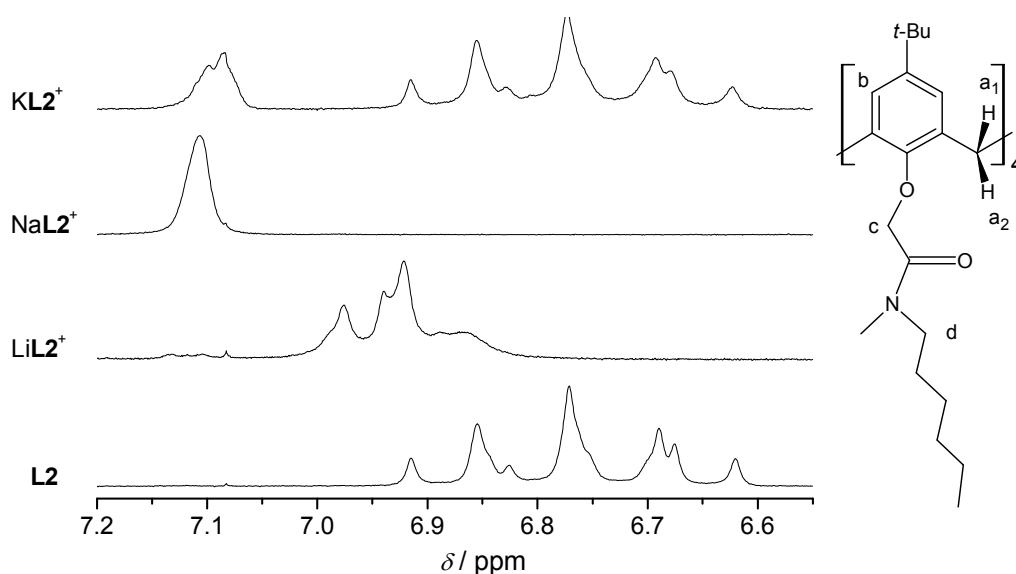
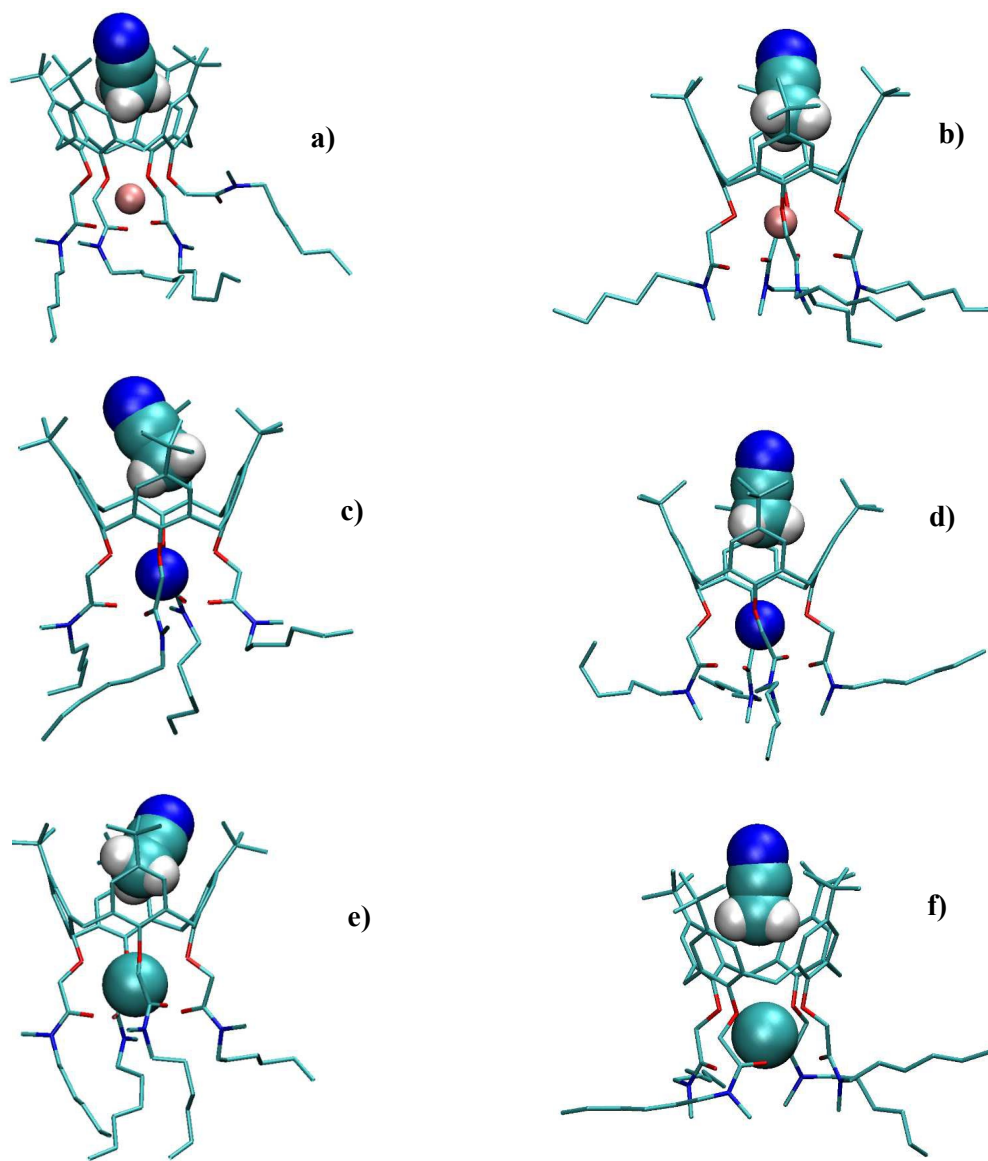


Fig. 8 ^1H NMR spectra of Ar-H protons of **L2**, LiL2^+ , NaL2^+ and KL2^+ in deuterated chloroform at 25 °C.

Molecular dynamics simulations of alkali metal cation complexes of **L1**, **E-L2** and **Z-L2** in acetonitrile rendered additional details about the molecular structures (Figs. 9, S16, and S17, ESI), binding site geometries and cation coordination, as well as the information on the process of solvent molecule inclusion in the calixarene hydrophobic cavity. During these simulations, alkali metal cations were coordinated by all four ether oxygen atoms and by variable number of carbonyl oxygen atoms (Tables S2–S3, S5–S8, ESI). The ligand-cation interaction energies in the complexes of **L1** and rotamers of **L2** were more favorable for smaller cations, whereby lithium cation was the most strongly bound to the calixarene ligands and cesium cation had the weakest interactions with these compounds. The coordination number of the cations depended on size as well. While lithium cation was coordinated by two carbonyl oxygen atoms on average, cesium was coordinated by nearly all four, owing to its large ionic radius. The distributions of distances between carbonyl-oxygen atoms and metal cations in the complexes are given in Figs. S18, S19, and S31–34, ESI. The inclusion of acetonitrile molecules in the hydrophobic cavities of complexes of **L1** and **L2** with alkali metal cations was more pronounced than in the cases of free ligands. Specifically bound MeCN molecule was present during most of the simulation time for all complexes, whereby 3 to 6 different molecules were exchanged during a single MD simulation. Upon the inclusion of the solvent molecule, the shape of calixarene *cone* became more regular. That was reflected by a decrease of the absolute

difference between the average values of the distances between opposite aromatic carbon atoms bound to *tert*-butyl groups and a referent distance for a pure *cone* shape (Tables S2–S4, S5–S8, ESI).²³ Also, the calixarene *cone* became more rigid when the hydrophobic cavity was filled with the solvent molecule, which was reflected by a decrease in the standard deviation of the distances between opposite aromatic carbon atoms bound to *tert*-butyl groups (Tables S2–S3, S5–S8, ESI). The interaction energy between specifically bound acetonitrile molecule and calixarene ligand was almost the same for all complexes of **L1** and **L2**, being around -50 kJ mol^{-1} .



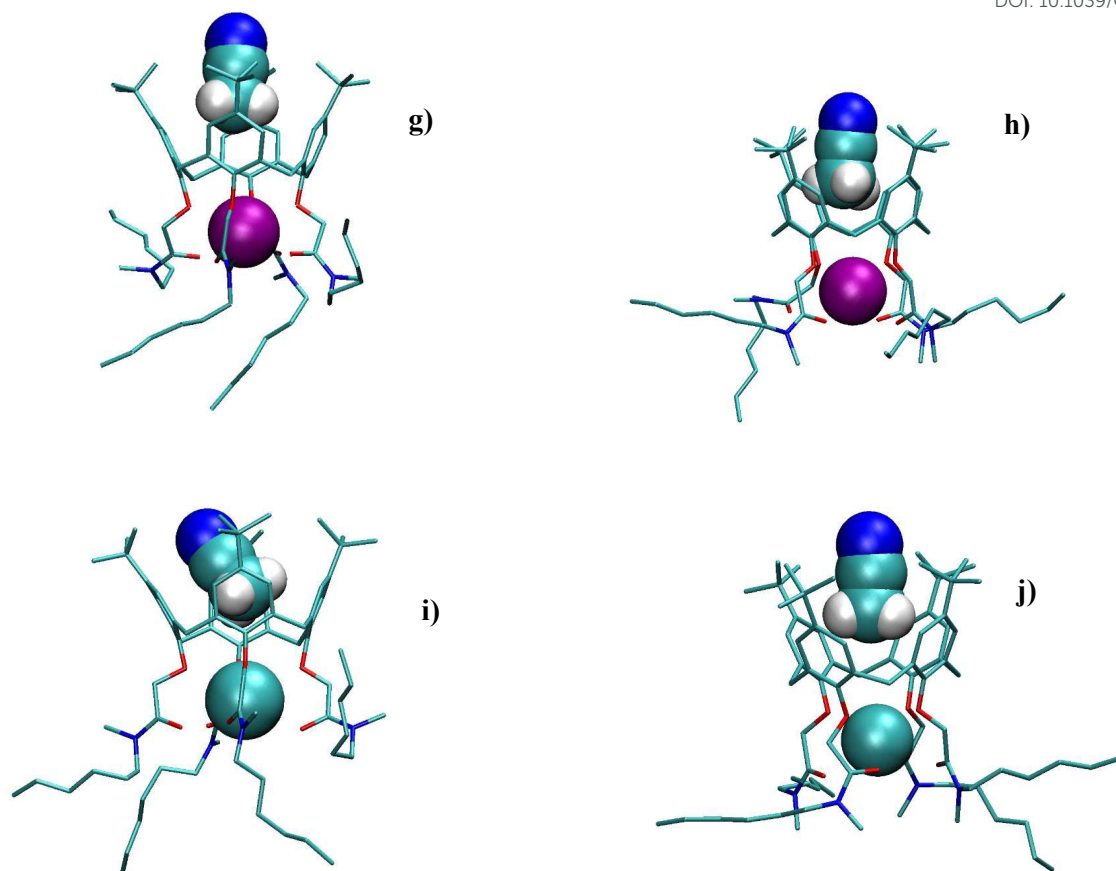


Fig. 9 Structures of a) LiZ-L2MeCN^+ , b) LiE-L2MeCN^+ , c) NaZ-L2MeCN^+ , d) NaE-L2MeCN^+ , e) KZ-L2MeCN^+ , f) KE-L2MeCN^+ , g) RbZ-L2MeCN^+ , h) RbE-L2MeCN^+ , i) CsZ-L2MeCN^+ and j) CsE-L2MeCN^+ obtained by MD simulations in acetonitrile at 25 °C. Hydrogen atoms are omitted for clarity.

3.4 Studies of alkali metal cations complexation in benzonitrile

The complexation reactions of ligands **L1** and **L2** with alkali metal cations were also studied in benzonitrile. We have already investigated the complexation of compound **L3** with Li^+ , Na^+ , and K^+ cations in benzonitrile, and have observed the coordination of metal cation by PhCN molecule included in the ligand hydrophobic *cone* in the case of LiL3^+ complex.¹⁶ In addition, we performed calorimetric titrations of calixarene-metal complexes with acetonitrile in benzonitrile by which the process of the inclusion of acetonitrile molecule in the calixarene *cone* was thermodynamically characterized.¹⁶

Like in acetonitrile, calixarenes **L1** and **L2** were shown to strongly bind most of the alkali metal cations in benzonitrile. The values of stability constants of the corresponding complexes, along with the reaction enthalpies and entropies, were determined by means of direct microcalorimetric titrations (CsL1^+ , RbL1^+ , CsL2^+ , RbL2^+ , KL2^+ , Figs. S37, S38, and S56–S58,

ESI) or by competition titration experiments (lithium, sodium, and potassium complexes of **L1** and **L2**, Fig. 10, S39, S40, S59, S60, ESI, and Table 2). The values of the reaction enthalpies for the reactions of **L1** with lithium, sodium, and potassium cations are lower about 5 kJ mol^{-1} in comparison to those of the complexation reactions of **L2** with the same cations. This effect, accompanied by the more favorable complexation entropies for the reactions of **L1**, results in the more stable complexes of LiL1^+ , NaL1^+ , and KL1^+ species with respect to the analogous complexes of ligand **L2**.

It should be noted that contrary to acetonitrile (where sodium complexes with **L1** and **L2** are the most stable), in benzonitrile both macrocycles show highest affinities towards Li^+ cation. The same was previously observed in the case of the derivative **L3** and accounted for by the favorable coordination of the smallest lithium cation by a nitrile nitrogen atom of the benzonitrile molecule included in the calixarene hydrophobic cone.¹⁶ The same arguments could be applied in the cases of **L1** and **L2** complexes (see also below).

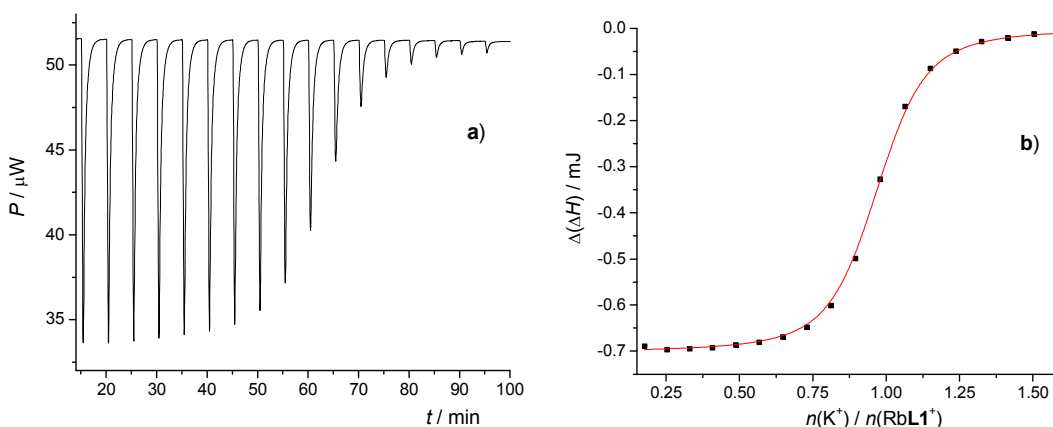


Fig. 10 a) Microcalorimetric titration of RbL1^+ ($c = 4.73 \times 10^{-4} \text{ mol dm}^{-3}$, $V = 1.4182 \text{ cm}^3$) with KSCN ($c = 3.33 \times 10^{-3} \text{ mol dm}^{-3}$) in benzonitrile; $t = 25 \text{ }^\circ\text{C}$; b) Dependence of successive enthalpy change on $n(\text{K}^+) / n(\text{RbL1}^+)$ ratio. ■ experimental; — calculated.

Table 2 Thermodynamic parameters for complexation of alkali metal cations with **L1** and **L2** in benzonitrile at 25 °C determined by direct and competitive microcalorimetric titrations.

Cation	$\log K \pm \text{SE}$	$(\Delta_r G^\circ \pm \text{SE})$ kJ mol ⁻¹	$(\Delta_r H^\circ \pm \text{SE})$ kJ mol ⁻¹	$(\Delta_r S^\circ \pm \text{SE})$ J mol ⁻¹ K ⁻¹
L1				
Li ⁺	11.86 ± 0.05	-67.7 ± 0.3	-51.6 ± 0.4	54 ± 2
Na ⁺	11.53 ± 0.02	-65.8 ± 0.1	-58.0 ± 0.2	26.0 ± 0.6
K ⁺	8.53 ± 0.02	-48.7 ± 0.1	-39.9 ± 0.2	29.4 ± 0.6
Rb ⁺	6.13 ± 0.02	-35.0 ± 0.1	-25.9 ± 0.2	30.4 ± 0.3
Cs ⁺	3.64 ± 0.02	-20.8 ± 0.1	-12.6 ± 0.5	27 ± 2
L2				
Li ⁺	10.68 ± 0.09	-61.0 ± 0.6	-46 ± 1	51 ± 5
Na ⁺	10.40 ± 0.05	-59.4 ± 0.3	-53.82 ± 0.7	18.8 ± 3
K ⁺	7.15 ± 0.05	-40.8 ± 0.3	-35.5 ± 0.7	18 ± 3
Rb ⁺	5.43 ± 0.01	-31.00 ± 0.05	-23.5 ± 0.2	25.3 ± 0.7
Cs ⁺	3.20 ± 0.07	-18.3 ± 0.4	-7.5 ± 0.1	36 ± 2

SE = standard error of the mean ($N = 3-5$).

3.5 Inclusion of acetonitrile molecule into the calixarene–cation complexes in benzonitrile

In order to study the inclusion of acetonitrile molecule in the hydrophobic *cone* of **L1** and **L2** complexes, the benzonitrile solutions of these complexes were microcalorimetrically titrated by the solution of MeCN in PhCN. It was reasonably (according to the complex stabilities) assumed that under the conditions used nearly all of the calixarene molecules were in the complexed form. As an example, titration of Na**L1**⁺ complex is shown in Fig. 11 (all other titrations are presented in Figs. S41–S43, ESI). The results of these titrations are presented in Table 3.

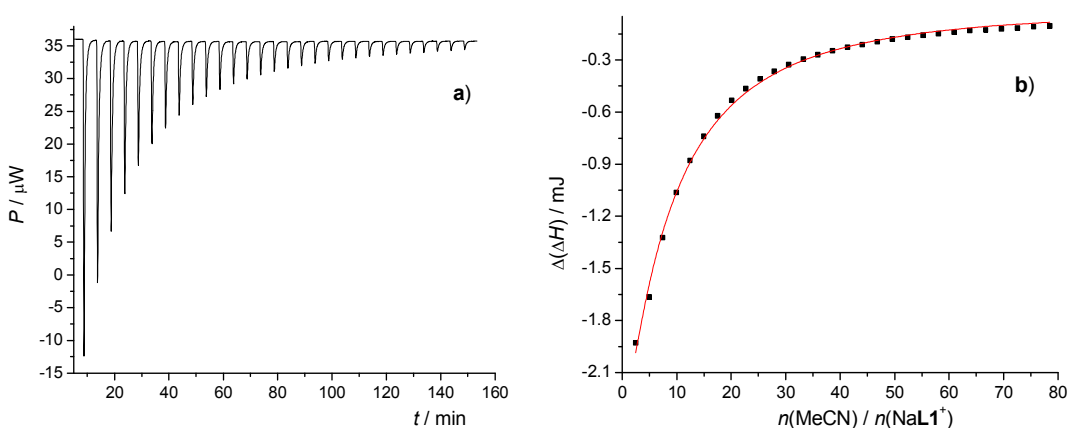


Fig. 11 a) Microcalorimetric titration of Na**L1**⁺ ($c = 2.90 \times 10^{-4} \text{ mol dm}^{-3}$, $V = 1.4182 \text{ cm}^3$) with MeCN ($c = 0.100 \text{ mol dm}^{-3}$) in benzonitrile; $t = 25 \text{ }^\circ\text{C}$; b) Dependence of successive enthalpy change on $n(\text{MeCN}) / n(\text{NaL1}^+)$ ratio. ■ experimental; — calculated.

Table 3 Thermodynamic parameters for the inclusion of acetonitrile in the complexes of **L1** and **L2** with alkali metal cations in benzonitrile at 25 °C determined by microcalorimetric titrations.

Complex	$\log K \pm \text{SE}$	$\frac{(\Delta_r G^\circ \pm \text{SE})}{\text{kJ mol}^{-1}}$	$\frac{(\Delta_r H^\circ \pm \text{SE})}{\text{kJ mol}^{-1}}$	$\frac{(\Delta_r S^\circ \pm \text{SE})}{\text{J mol}^{-1}\text{K}^{-1}}$
ML1⁺				
LiL1 ⁺	1.08 ± 0.01	-6.14 ± 0.05	-25.4 ± 0.2	-64.7 ± 0.4
NaL1 ⁺	2.266 ± 0.006	-12.94 ± 0.04	-43.8 ± 0.3	-103 ± 1
KL1 ⁺	1.955 ± 0.004	-11.16 ± 0.02	-47.1 ± 0.3	-121 ± 1
RbL1 ⁺	2.07 ± 0.01	-11.80 ± 0.06	-35.2 ± 0.3	-78 ± 1
ML2⁺				
LiL2 ⁺	1.015 ± 0.008	-5.80 ± 0.05	-25.1 ± 0.3	-65 ± 1
NaL2 ⁺	2.359 ± 0.007	-13.47 ± 0.04	-37.2 ± 0.2	-79.6 ± 0.7
KL2 ⁺	2.09 ± 0.01	-11.90 ± 0.06	-34.8 ± 0.5	-77 ± 2
RbL2 ⁺	1.981 ± 0.006	-11.30 ± 0.03	-31.2 ± 0.1	-66.7 ± 0.4

SE = standard error of the mean ($N = 3-5$).

Complexes LiL1⁺ and LiL2⁺ have almost the same affinity towards acetonitrile in benzonitrile, and this parity also holds for the corresponding values of reaction enthalpies and entropies. More pronounced differences in the affinities for MeCN molecule were found in the cases of sodium and potassium complexes. Although reaction enthalpies for the inclusion of acetonitrile in the *cave* of NaL1⁺ and KL1⁺ are more favorable than that for their L2 analogs, more negative reaction entropies in the cases of NaL1⁺ and KL1⁺ complexes eventually result in the lower stability of NaL1MeCN⁺ and KL1MeCN⁺ ternary species compared to that of NaL2MeCN⁺ and KL2MeCN⁺. It is interesting to note that stability constants of LiL1MeCN⁺ and LiL2MeCN⁺ species are an order of magnitude lower than those corresponding to acetonitrile adducts of L1 and L2 complexes with other alkali metal cations. This can be, at least partially, explained by taking into account already mentioned inclusion of benzonitrile molecule in the calixarene *cave*, previously observed in the case of LiL3⁺ complex.¹⁶ As an evidence of the benzonitrile inclusion in the lithium complexes can serve a comparison of reaction enthalpies and entropies of acetonitrile inclusion reactions (Table 3). The reaction enthalpies for the MeCN inclusion in the lithium complexes are less favorable than for the other complexes, which can be rationalized by considering the possibility of substitution of benzonitrile molecule included in the LiL1⁺ or LiL2⁺ *cave* by acetonitrile molecule. Such a substitution is most probably enthalpically less favorable than the inclusion of acetonitrile molecule in an unoccupied *cave*. Similar reasoning can be applied in the analysis in terms of entropy which is more favorable for the lithium L1 and L2 complexes compared to the others. That could be explained by taking into account that during the substitution process the loss of

acetonitrile translation entropy is compensated by the release of benzonitrile molecule bound to the calixarene *cone*.

To additionally confirm the importance of specific interaction with PhCN molecule, we calculated the $\Delta\Delta_t G^0$ values, *i.e.* the standard transfer Gibbs energies of sodium, potassium, and rubidium complexes relative to the standard transfer Gibbs energies of the corresponding lithium complexes, Eqs. (1 and 2):

$$\begin{aligned} \Delta\Delta_t G^0(\text{MLMeCN}^+(\text{MeCN}) \rightarrow \text{M-L}^+(\text{PhCN})) &= (\Delta_t G^0(\text{M}^+ + \text{L}, \text{PhCN}) - \Delta_t G^0(\text{M}^+ + \text{L}, \text{MeCN}) + \\ &+ \Delta_t G^0(\text{M}^+, \text{MeCN} \rightarrow \text{PhCN})) - (\Delta_t G^0(\text{Li}^+ + \text{L}, \text{PhCN}) - \Delta_t G^0(\text{Li}^+ + \text{L}, \text{MeCN}) + \Delta_t G^0(\text{Li}^+, \text{MeCN} \rightarrow \text{PhCN})) \end{aligned} \quad (1)$$

$$\begin{aligned} \Delta\Delta_t G^0(\text{MLMeCN}^+(\text{MeCN}) \rightarrow \text{MLMeCN}^+(\text{PhCN})) &= \Delta\Delta_t G^0(\text{MLMeCN}^+(\text{MeCN}) \rightarrow \text{M-L}^+(\text{PhCN})) + \\ &+ \Delta_t G^0(\text{M}^+ - \text{L} + \text{MeCN}, \text{PhCN}) - \Delta_t G^0(\text{Li}^+ - \text{L} + \text{MeCN}, \text{PhCN}) \end{aligned} \quad (2)$$

where M denotes Na, K, or Rb, M-L^+ corresponds to acetonitrile-free complexes with or without benzonitrile molecule included in the ligand *cone* whereas $\Delta_t G^0(\text{M}^+ + \text{L}, \text{solvent})$ and $\Delta_t G^0(\text{Li}^+ + \text{L}, \text{solvent})$ stand for the corresponding reaction Gibbs energies in the given solvent. The $\Delta_t G^0(\text{M}^+, \text{MeCN} \rightarrow \text{PhCN})$ values for Li^+ , Na^+ , K^+ and Rb^+ were calculated by combining the Gibbs energies of transfer of cations from water to acetonitrile⁵² or benzonitrile⁵³ based on $\text{Ph}_4\text{AsPh}_4\text{B}$ convention⁵⁴ ($\Delta_t G^0(\text{M}^+, \text{MeCN} \rightarrow \text{PhCN}) = \Delta_t G^0(\text{M}^+, \text{H}_2\text{O} \rightarrow \text{PhCN}) - \Delta_t G^0(\text{M}^+, \text{H}_2\text{O} \rightarrow \text{MeCN})$).

In that way, the standard transfer Gibbs energies of ligands **L1** and **L2** cancel out of the equation, and all conclusions are drawn based on comparison with the transfer of lithium-calixarene complexes. From the data listed in Table 4 it is evident that the $\Delta\Delta_t G^0(\text{MLMeCN}^+(\text{MeCN}) \rightarrow \text{M-L}^+(\text{PhCN}))$ values for all complexes are about 6 kJ mol^{-1} more positive than those corresponding to the $\text{MLMeCN}^+(\text{MeCN}) \rightarrow \text{MLMeCN}^+(\text{PhCN})$ transfer, relative to the transfer of lithium complex. The reason for these consistent differences can be assigned to the process of benzonitrile molecule inclusion which is most pronounced in the case of lithium complex and less expressed for the other alkali metal cation complexes of **L1** and **L2** in benzonitrile. In the above analysis it was assumed that all alkali metal cations complexes in MeCN are preferably in the form of acetonitrile adduct (Figs. 9, S16 and S17, ESI), as suggested by the results the MD simulations.

Table 4 Standard transfer Gibbs energies of sodium, potassium, and rubidium complexes relative to the standard transfer Gibbs energies of the corresponding lithium complexes (Eqs. 1 and 2).

Complex	$\frac{(\Delta\Delta_t G^\circ \pm SE)}{\text{kJ mol}^{-1}}$	$\frac{(\Delta\Delta_t G^\circ \pm SE)}{\text{kJ mol}^{-1}}$
	$\text{MLMeCN}^+(\text{MeCN}) \rightarrow \text{M-L}^+(\text{PhCN})$	$\text{MLMeCN}^+(\text{MeCN}) \rightarrow \text{MLMeCN}^+(\text{PhCN})$
L1		
NaL1 ⁺	7.0	0.2
KL1 ⁺	6.2	1.2
RbL1 ⁺	1.9	-3.8
L2		
NaL2 ⁺	8.3	0.6
KL2 ⁺	4.1	-2.0
RbL2 ⁺	-4.3	-9.8

In order to assess the molecular structures of alkali metal cation complexes of **L1** and **L2** ligands in benzonitrile, along with their affinities towards the inclusion of benzonitrile molecule, MD simulations were performed. During the simulations of the alkali metal cation complexes of **L1**, **E-L2** and **Z-L2** in benzonitrile the inclusion of solvent molecules was observed. In these adducts the included benzonitrile molecules were oriented in two different ways, one in which the nitrile group was pointing towards the bulk (structures denoted as MLPhCN^+ where M stands for the alkali metal cation and L is either **L1**, **E-L2** or **Z-L2** ligand), and the other where the nitrile group was inside the calixarene *cone* and oriented towards the alkali metal cation (denoted as MLPhCN^+). The presence of the latter adduct was more pronounced in the simulations of lithium and sodium complexes, but was also found in the simulations including other cations (Tables S9–S12 and S14–S21, ESI). The most favorable interaction between included benzonitrile molecule with a metal cation was that found for LiLPhCN^+ complexes followed by those of MLPhCN^+ type with sodium, potassium, and rubidium (Tables S9–S12 and S14–S21, ESI). Upon the coordination of cation by the nitrile group, in most cases an average number of coordinating carbonyl groups decreased. This was most evident for the NaL1⁺ and NaL2⁺ complexes where a reduction of the number of coordinating carbonyl groups resulted in an increase of the cation-ligand interaction energies by up to 40 kJ mol⁻¹ with respect to the same interaction in acetonitrile. As was the case for the acetonitrile adducts with alkali metal cation complexes of **L1**, **E-L2**, and **Z-L2**, the inclusion of benzonitrile molecule in the hydrophobic cavity resulted with a more rigid *basket* of more regular *cone* shape. Molecular dynamics simulations of MLMeCN^+ complexes in benzonitrile were also carried out in order to assess the structures and energetics of these species in this solvent. The compounds had similar interaction energies between complexed cations, ligands, and included acetonitrile molecules as the corresponding adducts in acetonitrile. As expected, the most pronounced difference was found in the solvation energies of the complexes in MeCN and PhCN.

3.6 Studies of alkali metal cation complexation in methanol

Complexation reactions of **L1** and **L2** were studied in methanol as well. This solvent was used because of its abilities of forming rather strong hydrogen bonds, both as proton donors and as proton acceptors. Complexation of alkali metal cations by **L1** and **L2** was followed by direct and competition microcalorimetric titrations (Table 5, Figs. S91–S94, S98–S101, ESI).

Table 5 Thermodynamic parameters for complexation of alkali metal cations with **L1** and **L2** in methanol at 25 °C determined by microcalorimetric titrations.

Cation	$\log K \pm \text{SE}$	$(\Delta_r G^\circ \pm \text{SE})$ kJ mol ⁻¹	$(\Delta_r H^\circ \pm \text{SE})$ kJ mol ⁻¹	$(\Delta_r S^\circ \pm \text{SE})$ J mol ⁻¹ K ⁻¹
L1				
Li ⁺	4.06 ± 0.03	-23.2 ± 0.2	-5.8 ± 0.1	58 ± 1
Na ⁺	7.78 ± 0.06	-44.5 ± 0.4	-45.9 ± 0.4	-5 ± 2
K ⁺	5.84 ± 0.05	-33.4 ± 0.3	-40.1 ± 0.4	-23 ± 2
Rb ⁺	3.77 ± 0.01	-21.50 ± 0.07	-21 ± 1	1 ± 4
L2				
Li ⁺	3.630 ± 0.004	-20.72 ± 0.02	-7.5 ± 0.2	44.3 ± 0.5
Na ⁺	7.33 ± 0.03	-41.9 ± 0.1	-45.6 ± 0.2	-13 ± 1
K ⁺	5.34 ± 0.01	-30.45 ± 0.07	-40.1 ± 0.2	-32.3 ± 0.6
Rb ⁺	3.22 ± 0.01	-18.36 ± 0.08	-22.1 ± 0.3	-13 ± 1

SE = standard error of the mean ($N = 3-5$).

To get more detailed thermodynamic information about the solvent effect on the reactions studied, an effort was made to determine the values of standard Gibbs energies of solution for **L1** and **L2** in acetonitrile and methanol. For that reason, the solubilities of the ligand in MeCN and MeOH were measured (Table 6). Standard solution Gibbs energies for methanol and acetonitrile as solvents were calculated from the solubility data using equation:

$$\Delta_{\text{sol}}G^\circ = -RT \ln K^\circ = -RT \ln(\gamma_{\text{L}} s/c^\circ) \approx -RT \ln(s/c^\circ) \quad (3)$$

where s denotes solubility, $c^\circ = 1 \text{ mol dm}^{-3}$ is standard concentration, and γ_{L} stands for the activity coefficient of the ligand which is assumed to be close to unity.

Table 6 Solubilities and derived standard solution Gibbs energies of **L1** and **L2** in acetonitrile and methanol at 25 °C.

	L1		L2	
	$10^3 \times s / \text{mol dm}^{-3}$	$\Delta_{\text{sol}}G^\circ / \text{kJ mol}^{-1}$	$10^3 \times s / \text{mol dm}^{-3}$	$\Delta_{\text{sol}}G^\circ / \text{kJ mol}^{-1}$
Acetonitrile	0.77	17.7	0.47	19.0
Methanol	16.1	10.2	40.4	8.0

The obtained values are reported in Table 6 and were used to calculate transfer Gibbs energies of LiL^+ , NaL^+ , KL^+ , RbL^+ and CsL^+ complexes from MeCN to MeOH (Schemes 2 and S2–S3) by the following equation:

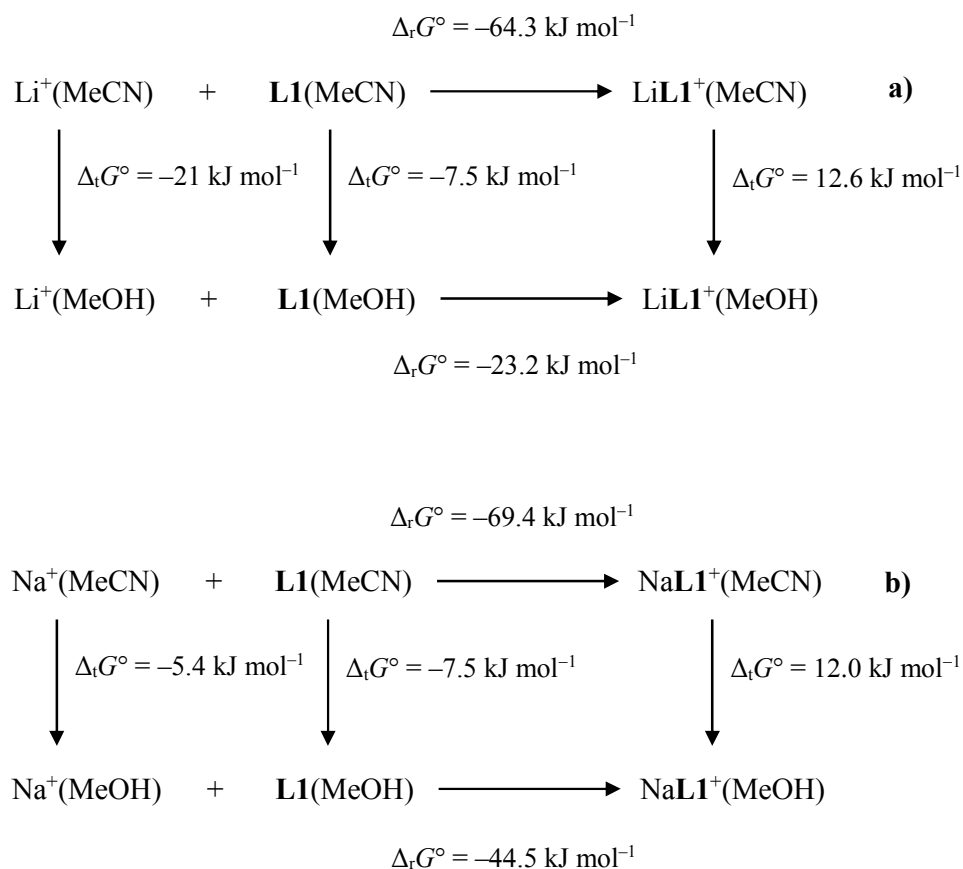
$$\Delta_{\text{t}}G^\circ(\text{ML}^+, \text{MeCN} \rightarrow \text{MeOH}) = \Delta_{\text{t}}G^\circ(\text{M}^+, \text{MeCN} \rightarrow \text{MeOH}) + \Delta_{\text{t}}G^\circ(\text{L}, (\text{MeCN} \rightarrow \text{MeOH})) + \Delta_{\text{r}}G^\circ(\text{MeOH}) - \Delta_{\text{r}}G^\circ(\text{MeCN}) \quad (4)$$

The $\Delta_{\text{t}}G^\circ(\text{M}^+, \text{MeOH} \rightarrow \text{MeCN})$ values for Na^+ and K^+ were calculated by combining the Gibbs energies of transfer of cations from water to methanol⁵² or acetonitrile⁵² based on $\text{Ph}_4\text{AsPh}_4\text{B}$ convention⁵⁴ ($\Delta_{\text{t}}G^\circ(\text{M}^+, \text{MeCN} \rightarrow \text{MeOH}) = \Delta_{\text{t}}G^\circ(\text{M}^+, \text{H}_2\text{O} \rightarrow \text{MeOH}) - \Delta_{\text{t}}G^\circ(\text{M}^+, \text{H}_2\text{O} \rightarrow \text{MeCN})$).

From the results presented in Table 5, a decrease of **L1** and **L2** affinities towards alkali metal cations is evident when compared to the stability of the corresponding complexes in acetonitrile and benzonitrile (Table 1 and **Table 2**). The origin of the effect from the thermodynamic point of view lies primarily in the favorable transfer Gibbs energies of **L1** and **L2** from acetonitrile to methanol (Schemes 2 and S1, S2, ESI) and in unfavorable transfer Gibbs energies of the ligand-cation complexes.

The impact of the differences in alkali metal cation solvation in the studied solvents (i.e. the corresponding transfer Gibbs energies) on the overall decrease in the affinities is not of great importance, except for lithium cation. In the latter case, the favorable cation transfer to methanol increases the standard Gibbs energy of complexation in methanol with respect to the one in acetonitrile as much as the sum of those of the free ligands and their complexes. Methanol is a proton-donating solvent which can form relatively strong hydrogen-bonding interactions with the carbonyl-oxygen atoms at the calixarene lower rim substituents. These interactions are the most likely cause of the favorable transfer of ligands **L1** and **L2** from acetonitrile to methanol. The increase in the Gibbs energies of solvation from acetonitrile to methanol of all calixarene-alkali metal cation complexes studied can be ascribed to the now missing interaction between carbonyl oxygen atoms and methanol molecules due to the cation coordination by the ligands carbonyl groups. In addition, an important contribution to the solvation of calixarene complexes in acetonitrile and methanol arises from the specific solvation, namely the inclusion of the solvent molecule in the

complexed calixarene *basket*. Such an interaction is more favorable in the case of acetonitrile inclusion,²³ thus having more beneficial effect on the overall complex stability.²³ When analyzing the contributions to standard Gibbs energy of complexation in acetonitrile and methanol, it can be seen that a decrease of the stability of **L1** and **L2** complexes is primarily influenced by the enthalpic contribution which is less favorable in methanol (Table 1, Table 2, and Table 5). Most of the complexes are stabilized by favorable reaction enthalpy except for the lithium ones where the favorable entropic contribution to the reaction Gibbs energy is quite significant. This finding can be related to the relatively high entropy of the lithium cation desolvation in methanol.



Scheme 2. Thermodynamic cycles for complexation of a) Li^+ and b) Na^+ with **L1** in acetonitrile and methanol expressed in terms of Gibbs energies.

Further insight into the structural aspects of the studied alkali metal cation complexes in methanol was obtained by molecular dynamics simulations of these compounds. The same conclusions can be drawn regarding the cation coordination and cation-ligand interaction energies as those presented above in the discussion of the results of MD simulations in acetonitrile. The most dominant form of all complexes in methanol was an MLMeOH^+ adduct which was present over 95 % of simulation time during every simulation (Tables S22–S26, ESI). The interaction energies

between the ligand and the included methanol molecule were around -50 kJ mol^{-1} in all of the observed adducts. Upon the inclusion of the solvent molecule, the calixarene *basket* became more regular and rigid, but this structural change did not influence the coordination of the cation, which remained the same as it was in the solvent-free complexes.

4. Conclusions

In this paper we present a thorough and systematic study of complexation of alkali metal cations by tertiary amide calix[4]arene derivatives **L1** and **L2** in acetonitrile, benzonitrile, and methanol. Thermodynamic quantities related to the studied reactions as well as MeOH→MeCN transfer Gibbs energies of reactants and products were determined.

The cation-binding affinities of **L1** and **L2** were found to be much higher than that of previously studied secondary-amide-based compound **L3**, which could be mostly ascribed to the presence of intramolecular hydrogen bonds formed between amide groups in the latter ligand (these bonds need to be disrupted in order to achieve ion binding). Compound **L1** comprising two hexyl groups bound to the amide nitrogen atom was proven to be better cation binder than **L2** with one methyl instead of hexyl, due to the better electron-donating ability of hexyl compared to methyl group, and hence higher basicity of the coordinating carbonyl oxygen atoms.

Most of the studied reactions were enthalpy driven. In some cases the favorable entropic contribution to the reaction Gibbs energy was quite significant, which was most likely related to the (de)solvation of the reactants and products of complexation reactions. Thermodynamic stabilities of the complexes generally decreased in the solvent order: MeCN > PhCN >> MeOH. Apart from the differences in the solvation of cations, ligands, and complexes, inclusion of solvent molecules in the calixarene hydrophobic cavity could also be responsible for this finding. The occurrence of this process was indicated by the results of ^1H NMR and MD studies, and was quantitatively characterized by means of isothermal titration calorimetry. In line with this, the highest affinities of **L1** and **L2** for Li^+ in benzonitrile (in other solvents stability peak corresponds to sodium cation) could be accounted for by considering the possibility of inclusion of solvent molecule in the calixarene *cone*, and coordination of this smallest cation by PhCN nitrile group.

5. Acknowledgments

This work has been fully supported by Croatian Science Foundation under the project IP-2014-09-7309 (SupraCAR). Computational resources provided by the Croatian National Grid Infrastructure (www.cro-ngi.hr) at Zagreb University Computing Centre (Sccc) were used for this publication.

References

1. Z. Asfari, V. Böhmer, J. Harrowfield and J. Vicens, Eds., *Calixarenes 2001*, Kluwer Academic Publishers, Dordrecht, 2001.
2. C. D. Gutsche, *Calixarenes: An Introduction*, The Royal Society of Chemistry, Cambridge, 2nd edn., 2008.
3. J. Vicens and J. Harrowfield, Eds., *Calixarenes in the Nanoworld*, Springer, Dordrecht, 2007.
4. A. F. Danil de Namor, R. M. Cleverley, and M. L. Zapata-Ormachea, *Chem. Rev.*, 1998, **98**, 2495–2526.
5. V. Böhmer, *Angew. Chemie Int. Ed. English*, 1995, **34**, 713–745.
6. A. Casnati, *Chem. Commun.*, 2013, **49**, 6827–6830.
7. W. Sliwa and T. Girek, *J. Incl. Phenom. Macrocycl. Chem.*, 2010, **66**, 15–41.
8. B. Mokhtari, K. Pourabdollah, and N. Dalali, *J. Incl. Phenom. Macrocycl. Chem.*, 2010, **69**, 1–55.
9. R. V Rodik, V. I. Boyko, and V. I. Kalchenko, *Curr. Med. Chem.*, 2009, **16**, 1630–1655.
10. B. S. Creaven, D. F. Donlon, and J. McGinley, *Coord. Chem. Rev.*, 2009, **253**, 893–962.
11. D. T. Schühle, J. a. Peters, and J. Schatz, *Coord. Chem. Rev.*, 2011, **255**, 2727–2745.
12. R. Ludwig and N. T. K. Dzung, *Sensors*, 2002, **2**, 397–416.
13. N. Bregović, N. Cindro, L. Frkanec, and V. Tomišić, *Supramol. Chem.*, 2016, **28**, 608–615.
14. I. Sviben, N. Galić, V. Tomišić, and L. Frkanec, *New J. Chem.*, 2015, **39**, 6099–6107.
15. A. F. Danil de Namor, T. T. Matsufuji-Yasuda, K. Zegarra-Fernandez, O. A. Webb, and A. El Gamouz, *Croat. Chem. Acta*, 2013, **86**, 1–19.
16. G. Horvat, V. Stilinović, B. Kaitner, L. Frkanec, and V. Tomišić, *Inorg. Chem.*, 2013, **52**, 12702–12.
17. J. Požar, G. Horvat, M. Čalogović, N. Galić, L. Frkanec, and V. Tomišić, *Croat. Chem. Acta*, 2012, **85**, 541–552.
18. J. Požar, T. Preočanin, L. Frkanec, and V. Tomišić, *J. Solution Chem.*, 2010, **39**, 835–848.
19. A. Hamdi, R. Abidi, and J. Vicens, *J. Incl. Phenom. Macrocycl. Chem.*, 2007, **60**, 193–196.
20. F. Arnaud-Neu, S. Barbosa, F. Berny, A. Casnati, N. Muzet, A. Pinalli, R. Ungaro, M.-J. Schwing-Weill, and G. Wipff, *J. Chem. Soc. Perkin Trans. 2*, 1999, 1727–1738.
21. F. Arnaud-Neu, G. Barrett, S. Fanni, D. Marrs, W. McGregor, M. A. McKervery, M.-J. Schwing-Weill, V. Vetrogon, and S. Wechsler, *J. Chem. Soc. Perkin Trans. 2*, 1995, **3**, 453–461.
22. A. Arduini, E. Ghidini, A. Pochini, R. Ungaro, G. D. Andreotti, G. Calestani, and F. Ugozzoli, *J. Incl. Phenom.*, 1988, **6**, 119–134.
23. G. Horvat, V. Stilinović, T. Hrenar, B. Kaitner, L. Frkanec, and V. Tomišić, *Inorg. Chem.*, 2012, **51**, 6264–6278.

24. A. F. D. de Namor, N. A. de Sueros, M. A. McKerverey, G. Barrett, F. A. Neu, and M. J. Schwing-Weill, *J. Chem. Soc. Chem. Commun.*, 1991, 1546–1548.
25. V. Tomišić, N. Galić, B. Bertoša, L. Frkanec, V. Simeon, and M. Žinić, *J. Incl. Phenom. Macrocycl. Chem.*, 2005, **53**, 263–268.
26. N. Galić, N. Burić, R. Tomaš, L. Frkanec, and V. Tomišić, *Supramol. Chem.*, 2011, **23**, 389–397.
27. T. Benković, V. Tomišić, L. Frkanec, and N. Galić, *Croat. Chem. Acta*, 2012, **85**, 469–477.
28. E. Nomura, M. Takagaki, C. Nakaoka, M. Uchida, and H. Taniguchi, *J. Org. Chem.*, 1999, **64**, 3151–3156.
29. L. Frkanec, A. Višnjevac, B. Kojić-Prodić, and M. Žinić, *Chem. Eur. J.*, 2000, **6**, 442–453.
30. A. F. Danil De Namor, W. B. Aparicio-Aragon, M. T. Goitia, and A. R. Casal, *Supramol. Chem.*, 2004, **16**, 423–433.
31. A. F. Danil de Namor, M. L. Zapata-Ormachea, and R. G. Hutcherson, *J. Phys. Chem. B*, 1999, **103**, 366–371.
32. M. T. Bakić, D. Jadreško, T. Hrenar, G. Horvat, J. Požar, N. Galić, V. Sokol, R. Tomaš, S. Alihodžić, M. Žinić, L. Frkanec, and V. Tomišić, *RSC Adv.*, 2015, **5**, 23900–23914.
33. A. S. de Araujo, O. E. Piro, E. E. Castellano, and A. F. Danil de Namor, *J. Phys. Chem. A*, 2008, **112**, 11885–11894.
34. P. Gans, A. Sabatini, and A. Vacca, *Talanta*, 1996, **43**, 1739–53.
35. J. Tellinghuisen, *J. Phys. Chem. B*, 2007, **111**, 11531–11537.
36. H. J. C. Berendsen, D. van der Spoel, and R. van Drunen, *Comput. Phys. Commun.*, 1995, **91**, 43–56.
37. E. Lindahl, B. Hess, and D. van der Spoel, *J. Mol. Model.*, 2001, **7**, 306–317.
38. D. Van Der Spoel, E. Lindahl, B. Hess, G. Groenhof, A. E. Mark, and H. J. C. Berendsen, *J. Comput. Chem.*, 2005, **26**, 1701–1718.
39. B. Hess, C. Kutzner, D. van der Spoel, and E. Lindahl, *J. Chem. Theory Comput.*, 2008, **4**, 435–447.
40. S. Pronk, S. Páll, R. Schulz, P. Larsson, P. Bjelkmar, R. Apostolov, M. R. Shirts, J. C. Smith, P. M. Kasson, D. van der Spoel, B. Hess, and E. Lindahl, *Bioinformatics*, 2013, **29**, 845–854.
41. S. Páll, M. J. Abraham, C. Kutzner, B. Hess, and E. Lindahl, in *Lecture Notes in Computer Science*, eds. S. Markidis and E. Laure, Springer, Cham, 2015, pp. 3–27.
42. M. J. Abraham, T. Murtola, R. Schulz, S. Páll, J. C. Smith, B. Hess, and E. Lindahl, *SoftwareX*, 2015, **1–2**, 19–25.
43. W. L. Jorgensen, D. S. Maxwell, and J. Tirado-Rives, *J. Am. Chem. Soc.*, 1996, **118**, 11225–11236.
44. W. C. Swope, H. C. Andersen, P. H. Berens, and K. R. Wilson, *J. Chem. Phys.*, 1982, **76**,

- 637–649.
45. T. Darden, D. York, and L. Pedersen, *J. Chem. Phys.*, 1993, **98**, 10089–10092.
 46. S. Nosé, *Mol. Phys.*, 1984, **52**, 255–268.
 47. W. Hoover, *Phys. Rev. A*, 1985, **31**, 1695–1697.
 48. G. J. Martyna, M. E. Tuckerman, D. J. Tobias, and M. L. Klein, *Mol. Phys.*, 1996, **87**, 1117–1157.
 49. W. Humphrey, A. Dalke, and K. Schulten, *J. Mol. Graph.*, 1996, **14**, 33–38.
 50. A. F. Danil de Namor, S. Chahine, E. E. Castellano, and O. E. Piro, *J. Phys. Chem. A*, 2005, **109**, 6743–6751.
 51. K. B. Wiberg, P. R. Rablen, D. J. Rush, and T. A. Keith, *J. Am. Chem. Soc.*, 1995, **117**, 4261–4270.
 52. Y. Marcus, *Ion Properties*, M. Dekker, New York, 1997.
 53. A. F. D. de Namor and H. B. de Ponce, *J. Chem. Soc. Faraday Trans. 1*, 1988, **84**, 1671–1678.
 54. J. Burgess, *Metal Ions in Solution*, Ellis Horwood, Chichester, 1978.